A Dual-Role Halogen-Bonding-Assisted EDA-SET/HAT Photoreaction System with Phenol Catalyst and Aryl Iodide: Visible-Light-Driven Carbon–Carbon Bond Formation

Tatsuhiro Uchikura, Kazushi Tsubono, Yurina Hara, Takahiko Akiyama

Department of Chemistry, Faculty of Science, Gakushuin University, 1-5-1, Mejiro, Toshima-ku, Tokyo 171-8588, Japan

KEYWORDS (Word Style "BG_Keywords"). If you are submitting your paper to a journal that requires keywords, provide significant keywords to aid the reader in literature retrieval.

ABSTRACT: Electron donor–acceptor (EDA) complex-mediated single-electron transfer (SET) is a crucial method for generating carbon radicals. Hydrogen atom transfer (HAT) enables the direct generation of alkyl radicals from alkanes. We report a dual-role EDA-SET/HAT photoreaction system for carbon–carbon bond formation using a phenol catalyst and aryl iodide. This system facilitates a Minisci-type addition of alkyl radicals to arenes. Mechanistic studies revealed that EDA complex formation is mediated by halogen bonding between phenoxide and aryl iodide. Irradiation of the EDA complex with visible light generates an aryl radical, which abstracts a hydrogen atom from an alkane to form an alkyl radical.

Carbon–carbon bond formation reactions are fundamental processes for the preparation of organic compounds. Among the numerous reactions developed to construct carbon skeletons, carbon radical addition is one of the most useful reactions because of its mild conditions.[1] Recently, reactions using carbon radical precursors under photoredox catalysis conditions have attracted much attention as such reactions can be performed with relatively low-energy visible light.[2] Moreover, since photosensitizers often contain expensive transition metal complexes such as iridium and ruthenium complexes, recent attention has been directed toward utilizing visible-light absorption promoted by substrate interactions.[3,4] A charge transfer interaction occurs between electron-rich and electron-deficient molecules, referred to as an electron donor–acceptor (EDA) complex.[5] Because EDA complexes often absorb visible light, irradiation of the EDA complexes promotes single-electron transfer (SET) to generate a radical ion pair. In recent years, carbon–carbon bond formation reactions based on EDA complex-mediated alkyl radical addition have been reported.[6] In these reactions, photosensitization is achieved using feedstocks without photosensitizers.

Reactive radical species such as phenyl radicals generated under photoredox catalysis conditions abstract hydrogen atoms from alkanes (hydrogen atom transfer: HAT) to generate alkyl radicals.[7] This process allows for the generation of alkyl radicals directly from alkanes instead of using the corresponding radical precursors. We envisioned that HAT reagents could be generated by excitation of EDA complexes in a reaction system that combines EDA-SET and HAT. In order to explore this strategy, we focused on phenols, i.e., feedstock compounds, as a catalyst (Figure 1a) since their conjugate bases (phenoxides) are stable anionic species known to serve as electron donors in EDA complex formation via π–π stacking or halogen bonding.[8] Several groups employed phenoxide/aryl halide EDA complex formation for the light-driven C–O[9] or C–C[10] bond formation reactions (Figure 1b).

We have recently reported an EDA-SET/HAT combined system for light-driven C–S bond formation via aryl radical generation using aryl halides (Figure 1c), in which hydrogen atom abstraction from alkanes by aryl radicals led to generation of alkyl radicals.[11] We hypothesized that the use of electron donors that generate more stable radical species via SET may allow for the generation of alkyl radicals that can react with other radical acceptors.

Here we report an EDA-SET/HAT combined system for visible-light-driven C–C bond formation between arenes and alkanes using phenol as a catalyst, with subsequent aryl radical generation (Figure 1d). Electron-deficient arenes or heteroarenes can be used as radical acceptors.[12] In addition, we demonstrate that the formation of the phenoxide/aryl iodide EDA complex is mediated by halogen bonding on the basis of experimental and theoretical studies.

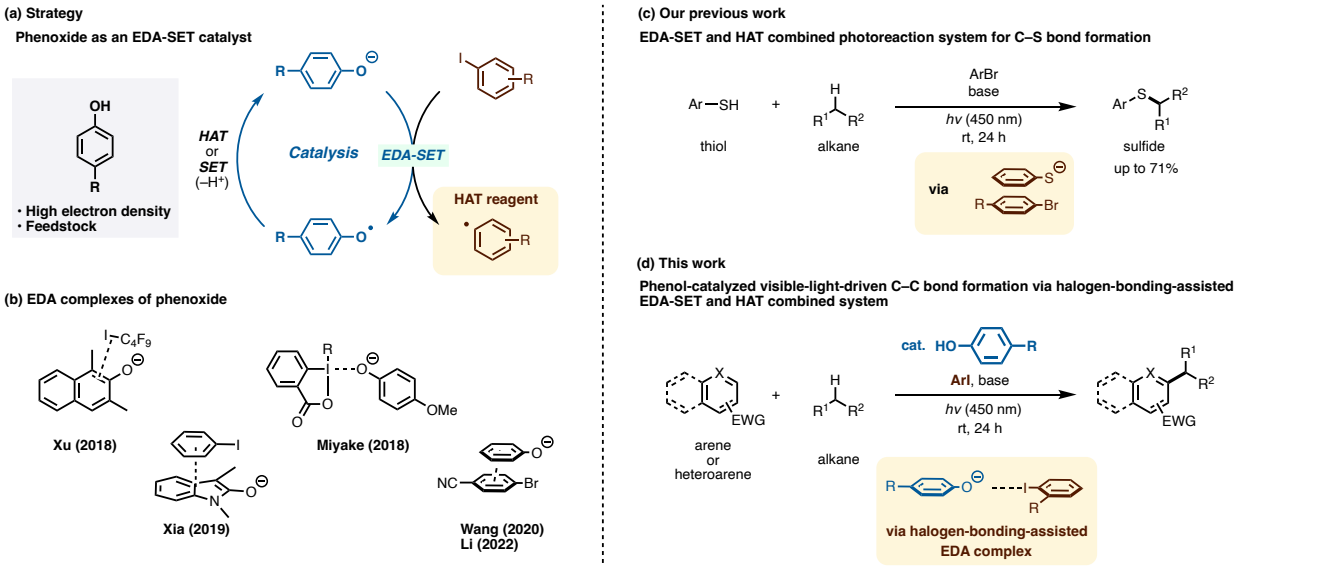

Figure 1. Background and strategy of this study.

We initially examined the reaction of 2-naphthonitrile (**1a**) and tetrahydrofuran (THF, **2a**) in the presence of a catalytic amount of *p-tert*-butylphenol (**3a**), 2.0 equiv of *o*-fluoroiodobenzene (**4a**), and 5 equiv of cesium carbonate in DMSO under photoirradiation conditions. This reaction led to C–C bond formation at 1-position to give **5a** in 81% yield (Table 1, entry 1). The screening of phenol catalysts revealed that **3a** is the most efficient in generating **5a** (entries 2–4).

When 2-chloroiodobenzene (**4b**) was used in place of **4a**, the yield of **5a** slightly decreased to 73% (entry 5). The use of **4c**, a more electron-deficient aryl halide, further reduced the yield of **5a** to 53%, as the reaction was accompanied by the formation of **5p**, a coupling product of the THF radical and dehalogenated aryl halide (entry 6). Use of dimethyl sulfoxide as a solvent and cesium carbonate as a base was the best conditions (entries 7–12). Lowering **2a** to 20 equivalents afforded **5a** in 71% yield (entry 13).

Control experiments showed that a phenol catalyst, aryl halide, base, and photoirradiation were crucial for the reaction to take place (entries 14–17). Moreover, the reaction proceeded only under degassed conditions (entry 18).[13, 14]

Table 1. Screening of conditions[a)]

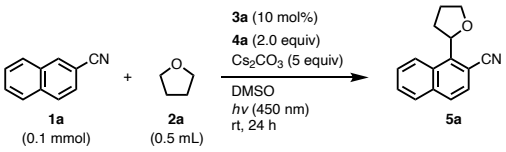

Entry	Deviation from the standard conditions	Yield[b)]
1	None	81%[c)]
2	**3b** instead of **3a**	58%
3	**3c** instead of **3a**	53%
4	**3d** instead of **3a**	56%
5	**4b** instead of **4a**	73%[c)]
6	**4c** instead of **4a**	53%
7	DMF instead of DMSO	30%
8	CH_3CN instead of DMSO	40%
9	K_2CO_3 instead of Cs_2CO_3	8%
10	^{t}BuOK instead of Cs_2CO_3	42%
11	CsOH instead of Cs_2CO_3	51%
12	KOH instead of Cs_2CO_3	39%
13	Using 20 equiv of **2a**	71%[c)]
14	Without **3a**	16%
15	Without **4a**	0%
16	Without Cs_2CO_3	0%
17	Without irradiation	0%
18	Under air	0%

(a) Performed with **1a** (0.10 mmol), **2a** (0.5 mL), **3a** (0.010 mmol), **4a** (0.15 mmol), and Cs_2CO_3 in DMSO (0.5 mL) under irradiation with 450 nm blue LEDs. (b) Determined by ^{1}H NMR (1,1,2-trichloroethane was used as an internal standard). (c) Isolated yield. DMSO, dimethyl sulfoxide; DMF, *N,N*-dimethylformamide.

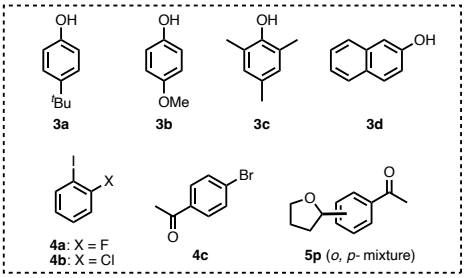

The substrate scope of arenes **1** was investigated under the optimized conditions (Figure 2). 1-Naphthonitrile (**1b**) gave 4-alkylated product **5b** in 63% yield. 1-Acetyl and methoxycarbonyl naphthalenes (**1c**, **1d**) were also suitable, generating coupling products **5c** and **5d**, respectively, in moderate yields. Simple arenes such as naphthalene (**1e**) and pyrene (**1f**) also afforded the desired products (**5e, 5f**) in modest yields. Benzonitrile (**1g**) underwent the addition reaction of the THF radical at both *ortho*- and *para*- positions, giving **5g** in 42% yield (*o*:*p* = 17:25), whereas *para*-substituted benzonitriles (**1h**–**1o**) gave coupling products (**5h**–**5o**) only at the *ortho*-position relative to the cyano group. Use of electron-deficient

substrates (**1h**, **1i**) resulted in the formation of **5h** and **5i** in modest yields accompanied by di-substitution products. In contrast, *p*-methylbenzonitrile (**1j**) gave **5j** in as low as 19% yield. Acetophenone (**1p**) and benzophenone (**1q**) yielded adducts **5p** (30%) and **5q** (41%), respectively, and 1,4-dicarbonyl compounds (**1r**, **1s**) yielded single adducts **5r** (26%) and **5s** (44%), respectively. Heteroarenes (**1t**–**1x**) were also applicable: quinoline, quinoxaline, isoquinoline, and electron-deficient pyridine furnished THF adducts **5t**–**5x** in moderate yields. Furthermore, benzothiazole (**1y**) and benzoxazole (**1z**) reacted with the THF radical at 2-position to yield **5y** (57%) and **5z** (30%), respectively.

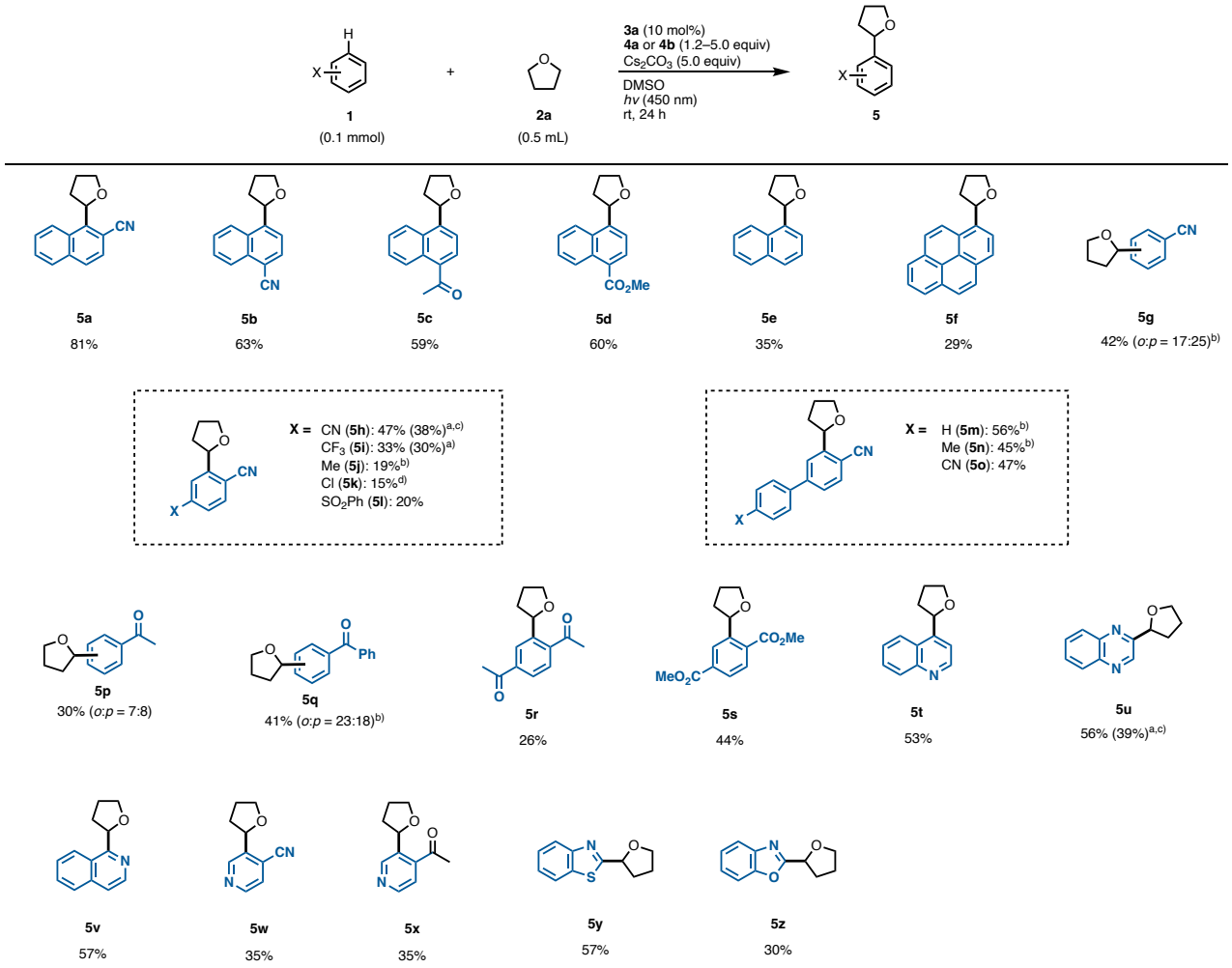

a) Dialkylated products were obtained (yields shown in parenthesis).
b) KOH was used as a base instead of Cs_2CO_3.
c) The reaction was run for 12 h.
d) Dechlorinated product was obtained in 59% yield.

Figure 2. Substrate scope

Next, we investigated the generality of alkanes **2** (Figure 3). Cyclic ethers such as tetrahydropyran (**2b**), 1,4-dioxane (**2c**), 1,3-dioxolane (**2d**), and 2,2-dimethyl-1,3-dioxolane (**2e**) were applicable as substrates, generating coupling products (**6b**–**6e**) in moderate yields. Acyclic ethers were also applicable: diethyl ether (**2f**) and 1,2-dimethoxyethane (**2g**) gave **6f** and **6g**, respectively, in low to moderate yields. Tetrahydrothiophene (**2h**), a sulfide, afforded **6h** albeit in low yield. Cyclic amides *N*,*N*′-dimethylimidazolidinone (**2i**) and *N*-methylpyrrolidone (**2j**) afforded **6i** and **6j**, respectively. Notably, cyclopentane (**2k**), a simple hydrocarbon, was also applicable, giving **6k** in 31% yield. Trioxane, when reacted with **1a** and **1d**, generated **6l** and **6m** in 40% and 30% yield, respectively.

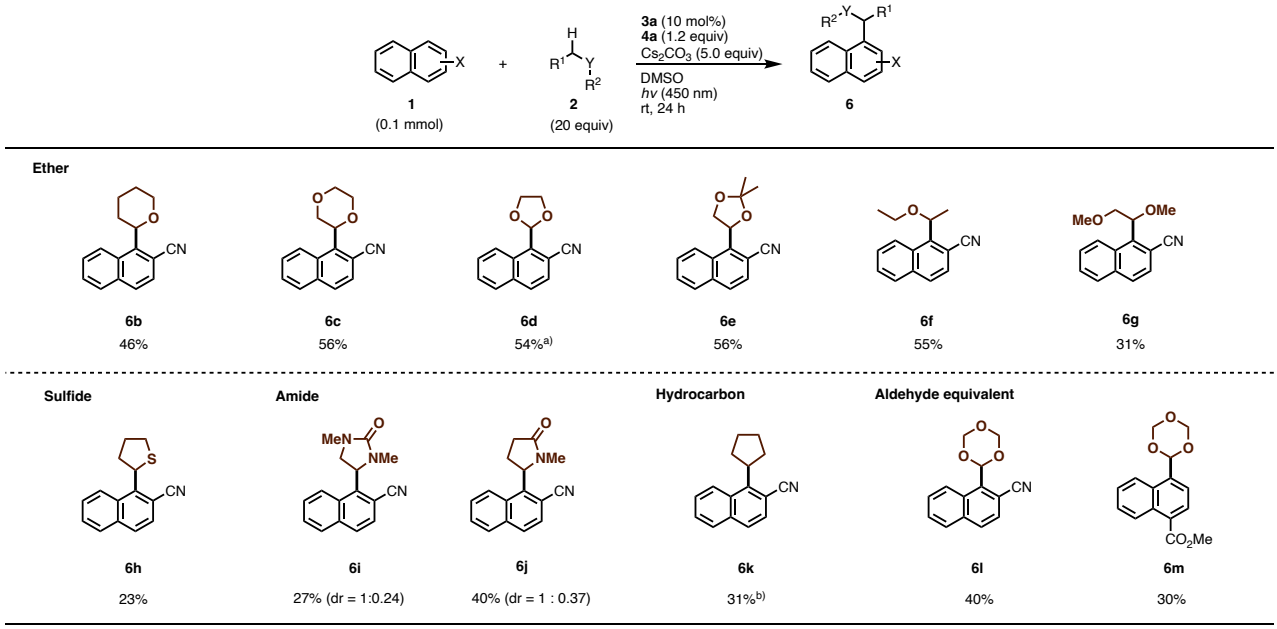

a) 17% of by-product was obtained.
b) 0.5 mL of **2** was used.

Figure 3. Generality of alkyl and acyl groups.

Furthermore, **6m** could be derivatized into methyl 4-formyl-1-naphthoate (**7**) in 96% yield, suggesting that the reaction could be applied to C–H formylation reactions as well (Scheme 1).[15]

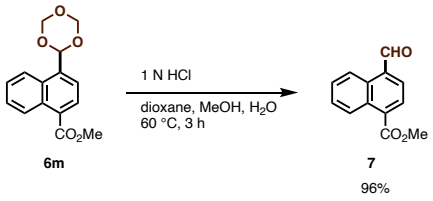

Scheme 1. Hydrolysis of trioxane derivative 6m to form aldehyde 7.

Finally, mechanistic studies of the present reaction system were carried out. The inhibition of C–C bond formation by the addition of free radical scavengers, such as *N*-*tert*-butyl-α-phenylnitrone (PBN) and 2,2,6,6-tetramethylpiperidine-1-oxyl (TEMPO), conclusively supported a radical pathway (Figure 4a). Moreover, the use of THF-d_8 instead of THF under the optimized conditions (shown in Figure 2) led to the formation of 2-deuterated chlorobenzene, as confirmed by ^{2}H NMR measurements,[16] suggesting that the generation of 2-chlorophenyl radical followed by the abstraction of the hydrogen atom from THF (Figure 4b). Furthermore, in order to determine the rate-determining step of the reaction, the kinetic isotope effect (KIE) was estimated using a 1:1 mixture of THF and THF-d_8. A positive KIE (k_H/k_D = 3.1) was observed, and the HAT process was suggested to be the rate-determining step (Figure 4c). The calculated quantum yield of the reaction was Φ = 0.045, supporting a photoinduced pathway (Figure 4d).[17]

EDA complex formation was confirmed from the UV–vis spectra, which showed an increase in absorbance at 400–500 nm when **4b** and sodium *p*-*tert*-butylphenoxide (**3a-Na**) were mixed (Figure 4e).[18] The Job plot analysis of the EDA complex **3a-Na**/**4b** at 420 nm yields a 1:1 ratio of the two components form a 1:1 EDA (Figure 4f).[19]

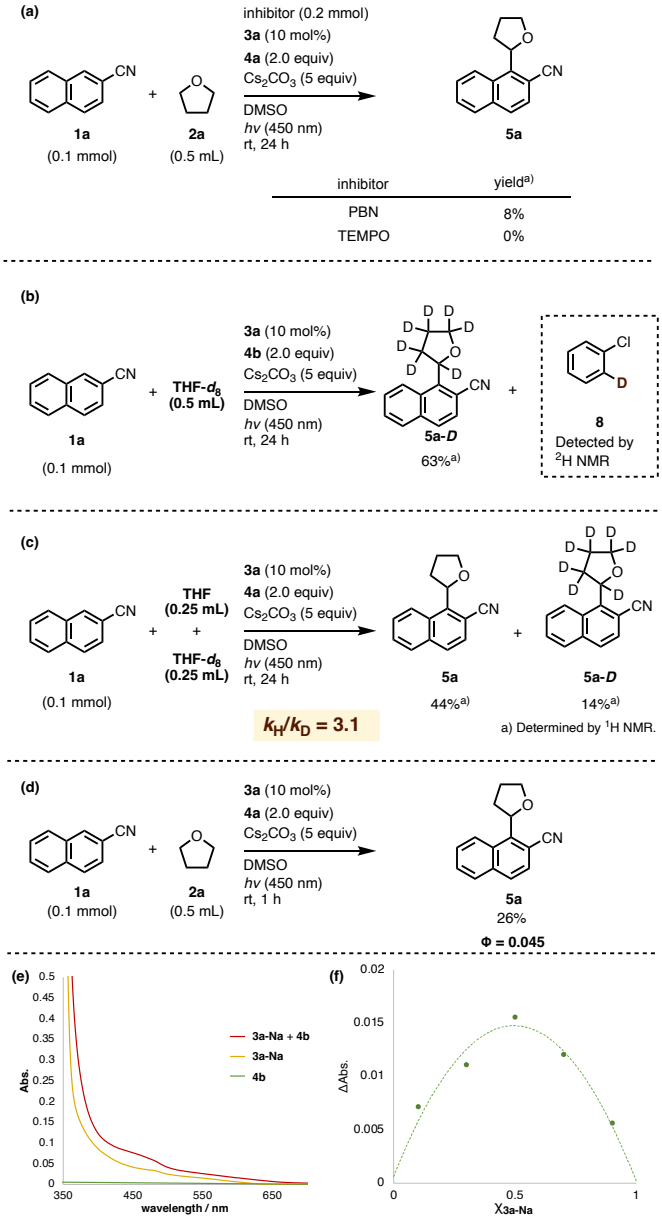

Figure 4. Mechanistic studies. (a) Addition of free radical scavengers. (b) Deuterium labeling experiment. (c) Kinetic isotope effect measurement. (d) Quantum yield determination. (e) UV–vis spectra of 3a and 4b. (f) Job plot of the EDA complex (UV-vis absorption at 420 nm).

This 1:1 EDA complex can exist in two possible forms, one mediated by halogen bonding and the other, by π–π stacking (Figure 5). To determine the structure of the complex, we investigated whether the reaction would proceed in the presence of inhibitors that block the respective interactions (Figure 6a). The addition of 2-methoxynaphthalene, a π–π stacking inhibitor, slightly inhibited the formation of **5a**, whereas nonafluoro-1-iodobutane, a halogen bonding inhibitor, significantly inhibited the formation of **5a**.

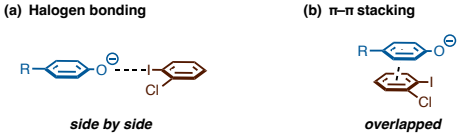

Figure 5. Two possible forms of the EDA complex between 3a and 4b.

We then performed ^{1}H NMR experiments to directly observe EDA complex formation between *p-tert*-butylphenoxide and **4b**. The formation of a "side-by-side" complex via halogen bonding (Figure 5a) would result in a shift of the ^{1}H NMR signals to lower field compared with those of free components because of the anti-shielding effects of the aromatic rings. On the other hand, the signals of the "overlapped" EDA complex via π–π stacking (Figure 5b) would shift to higher field because of the shielding effects of the aromatic rings. In the presence of **4b**, the peaks of phenoxide aromatic protons shifted to lower field (Figure 6b). The proton signals of **4b** was shifted to higher field as the amount of **4b** increased. To put it another way, that signals was shifted to lower field as increasing the ratio of phenoxide. These findings suggest that the two aromatic rings were positioned "side by side," and that the formation of the EDA complex is mediated by halogen bonding under the present reaction conditions.

In order to obtain further evidence, we performed density functional theory (DFT) calculations for the two forms of the EDA complex. ΔG of the halogen-bonding-assisted EDA complex was 0 kcal·mol^{-1}, whereas that of the π–π stacking-assisted EDA complex was 3.9 kcal·mol^{-1}, suggesting that the former is more stable than the latter (Figure 6c).[20]

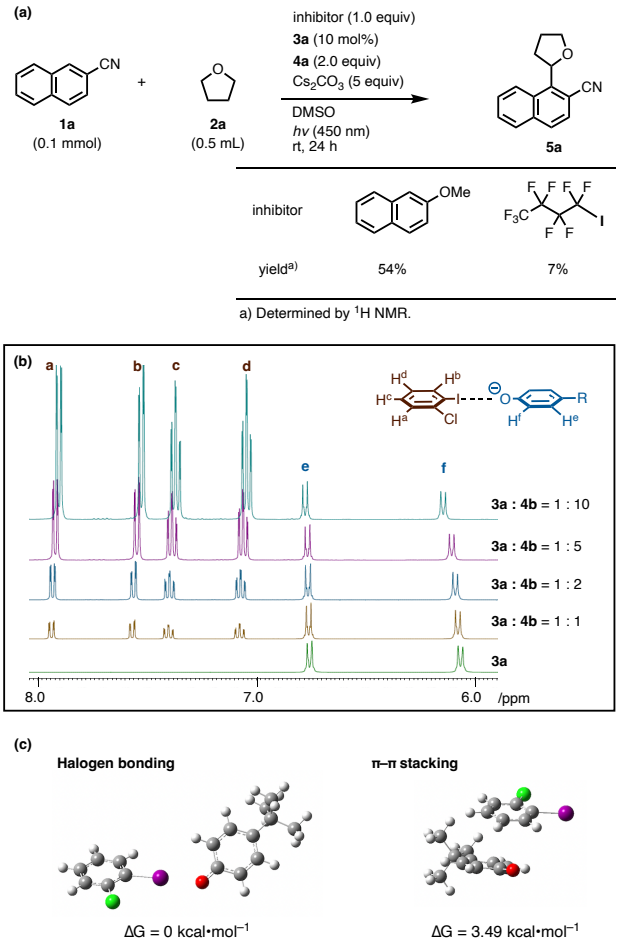

Figure 6. Determination of EDA complex structure. (a) Addition of the inhibitors of EDA complex formation. (b) ^{1}H NMR spectra of the EDA complex between 3a and 4b. (c) DFT

calculations for the two forms of the EDA complex (APFD/DGDZVP).

The proposed mechanism of the present reaction system based on the results of mechanistic studies is shown in Figure 7. A phenoxide, generated from the reaction of a phenol catalyst and base, forms an EDA complex with iodoarene via halogen bonding. Visible-light excitation of the EDA complex generates phenoxy and aryl radicals. Subsequently, the aryl radical acting as a HAT reagent abstracts an alkane hydrogen atom to generate an alkyl radical, followed by a Minisci-type radical addition to an arene. The hydrogen atom in radical intermediate **A** is abstracted by the phenoxy radical to generate product **5**, and the phenoxide ion is regenerated by deprotonation.

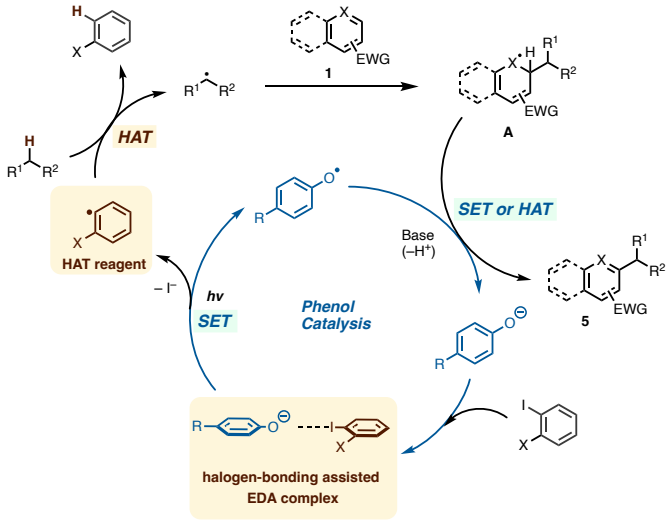

Figure 7. Proposed mechanism.

We developed a phenoxide-catalyzed visible-light-driven radical C–C bond formation reaction using a combined system of EDA-SET and HAT. Various alkyl radicals including those from simple alkanes were formed by this method. Mechanistic studies revealed that aryl radicals, generated by EDA complex excitation, abstract hydrogen atoms from alkanes, resulting in the formation of alkyl radicals. Experimental and theoretical studies revealed that the formation of the EDA complex is mediated by halogen bonding between phenoxide and aryl iodide. This photoreaction system requires only feedstock reagents and not expensive catalysts or highly reactive compounds. We believe that this simple and readily available radical generation system combining EDA-SET and HAT will find applications in other types of radical reactions.

ASSOCIATED CONTENT

Supporting Information

The Supporting Information is available free of charge at http://pubs.acs.org/doi/10.1021/acscatal.xxxx.
Additional table of optimization data, experimental procedures, compounds characterization data, and mechanistic studies (PDF)

AUTHOR INFORMATION

Corresponding Author

Takahiko Akiyama – *Department of Chemistry, Faculty of Science, Gakushuin University, 1-5-1, Mejiro, Toshima-ku, Tokyo 171-8588, Japan;*
ORCID: 0000-0003-4709-4107
Email: takahiko.akiyama@gakushuin.ac.jp

Authors

Tatsuhiro Uchikura – *Department of Chemistry, Faculty of Science, Gakushuin University, 1-5-1, Mejiro, Toshima-ku, Tokyo 171-8588, Japan;*
ORCID: 0000-0002-0327-3675
Email: tatsuhiro.uchikura@gakushuin.ac.jp

Kazushi Tsubono – *Department of Chemistry, Faculty of Science, Gakushuin University, 1-5-1, Mejiro, Toshima-ku, Tokyo 171-8588, Japan*

Yurina Hara – *Department of Chemistry, Faculty of Science, Gakushuin University, 1-5-1, Mejiro, Toshima-ku, Tokyo 171-8588, Japan*

Funding Sources

JSPS KAKENHI Grant numbers, JP20H00380, and JP20H04826 (Hybrid Catalysis) for T. A. JSPS KAKENHI Grant number, JP20K15287 for T. U.

ACKNOWLEDGMENT

We thank Prof. Masahiro Yamanaka (Rikkyo University) for discussion about DFT calculation.

REFERENCES

[1] For recent reviews on radical addition, see: (a) Studer, A.; Curran, D. P. Catalysis of Radical Reactions: A Radical Chemistry Perspective. *Angew. Chem. Int. Ed.* **2016**, *55*, 58-102. (b) Proctor, R. S. J.; Phipps, R. J. Recent Advances in Minisci-Type Reactions. *Angew. Chem. Int. Ed.* **2019**, *58*, 13666–13699. (c) Crespi, S. Fagnoni, M. Generation of Alkyl Radicals: From the Tyranny of Tin to the Photon Democracy. *Chem. Rev.* **2020**, *120*, 9790–9833. (d) Kanegusuku, A. L. G.; Roizen, J. L. Recent Advances in Photoredox-Mediated Radical Conjugate Addition Reactions: An Expanding Toolkit for the Giese Reaction. *Angew. Chem. Int. Ed.* **2021**, *60*, 21116–21149. (e) Kitcatt, D. M.; Nicolle, S.; Lee, A.-L. Direct Decarboxylative Giese Reactions. *Chem. Soc. Rev.* **2022**, *51*, 1415–1453. (f) Huang, C.-Y.; Li, J.; Li, C.-J. Photocatalytic C(sp^3) Radical Generation via C–H, C–C, and C–X Bond Cleavage. *Chem. Sci.* **2022**, *13*, 5465–5504

[2] For recent reviews on photoreactions, see: (a) Prier, C. K.; Rankic, D. A.; MacMillan, D. W. C. Visible Light Photoredox Catalysis with Transition Metal Complexes: Applications in Organic Synthesis. *Chem. Rev.* **2013**, *113*, 5322–5363. (b) Romero, N. A.; Nicewicz, D. A. Organic Photoredox Catalysis. *Chem. Rev.* **2016**, *116*, 10075–10166. (c) Shaw, M. H.; Twilton, J.; MacMillan, D. W. C. Photoredox Catalysis in Organic Chemistry. *J. Org. Chem.* **2016**, *81*, 6898–6926. (d) Ravelli, D.; Protti, S.; Fagnoni, M. Carbon–Carbon Bond Forming Reactions via Photogenerated Intermediates. *Chem. Rev.* **2016**, *116*, 9850–9913. (e) Michelin, C.; Hoffmann, N. Photosensitization and Photocatalysis–Perspectives in Organic Synthesis. *ACS Catal.* **2018**, *8*, 12046–12055. (f) Glaser, F.; Kerzig, C.; Wenger, O. S. Multi-Photon Excitation in Photoredox Catalysis: Concepts, Applications, Methods. *Angew. Chem. Int. Ed.* **2020**, *59*, 10266–10284. (g) Regotti, T.; Alemán, J. Visible Light Photocatalysis – From Racemic to Asymmetric Activation Strategies. *Chem. Commun.* **2020**, *56*, 11169–11190. (h) Amos, S. G. E.; Garreau, M.; Buzzetti, L.; Waser, J. Photocatalysis with Organic Dyes: Facile Access to Reactive Intermediates for Synthesis. *Beilstein J. Org. Chem.* **2020**, *16*, 1163–1187. (i) Ganley, J. M.; Murray, P. R. D.; Knowles, R. R. Photocatalytic Generation of Aminium Radical Cations for C–N Bond Formation.*ACS Catal.* **2020**, *10*, 11712–11738. (j) Li, H.; Liu, Y.; Chiba, S. Leveraging of Sulfur

Anions in Photoinduced Molecular Transformations. *JACS Au* **2021**, *1*, 2121–2129. (k) Schmalzbauer, M.; Marcon, M.; König, B. Excited State Anions in Organic Transformations. *Angew. Chem. Int. Ed.* **2021**, *60*, 6270–6292.

[3] Sumida, Y. ; Ohmiya, H. Direct Excitation Strategy for Radical Generation in Organic Synthesis. *Chem. Soc. Rev.* **2021**, *50*, 6320–6332.

[4] We recently reported enantioselective alkyl radical addition by direct excitation of chiral phosphoric acid-imine complex, see: Uchikura, T.; Kamiyama, N.; Mouri, T.; Akiyama, T. Visible-Light-Driven Enantioselective Radical Addition to Imines Enabled by the Excitation of a Chiral Phosphoric Acid–Imine Complex. *ACS Catal.* **2022**, *12*, 5209–5216.

[5] For reviews on EDA complex, see: (a) Foster, R. Electron Donor-Acceptor Complexes. *J. Phys. Chem.* **1980**, *84*, 2135–2141. (b) Rosokha, S. V.; Kochi, J. K. Fresh Look at Electron-Transfer Mechanism via the Donor/Acceptor Bindings in the Critical Encounter Complex. *Acc. Chem. Res.* **2008**, *41*, 641–653. (c) Emmett, L.; Prentice, G. M.; Dan Pantoş, G. Donor-Acceptor Interactions in Chemistry. *Annu. Rep. Prog. Chem., Sect. B: Org. Chem.* **2013**, *109*, 217–234. (d) Crisenza, G. E. M.; Mazzarella, D.; Melchiorre, P. Synthetic Methods Driven by the Photoactivity of Electron Donor–Acceptor Complexes. *J. Am. Chem. Soc.* **2020**, *142*, 5461–5476. (e) Yuan, Y.-q.; Majumder, S.; Yang, M.-h.; Guo, S.-r. Recent Advances in Catalyst-Free Photochemical Reactions via Electron-Donor-Acceptor (EDA) Complex Process. *Tetrahedron Lett.* **2020**, *61*, 151516. (f) Yang, Z.; Liu, Y.; Cao, K.; Zhang, X.; Jiang, H.; Li, J. Synthetic Reactions Driven by Electron-Donor-Acceptor (EDA) Complexes. *Beilstein J. Org. Chem.* **2021**, *17*, 771–799. (g) Zhang, L.; Cai, L.; Tao, K.; Xie, Z.; Lai, Y.-L.; Guo, W. Progress in Photoinduced Radical Reactions using Electron Donor-Acceptor Complexes. *Asian J. Org. Chem.* **2021**, *10*, 711–748.

[6] For recent reports on photoreactions via formation of EDA complex, see: (a) de Pedro Beato, E.; Spinnato, D.; Zhou, W.; Melchiorre, P. A General Organocatalytic System for Electron Donor-Acceptor Complex Photoactivation and Its Use in Radical Processes. *J. Am. Chem. Soc.* **2021**, *143*, 12304–12314. (b) Yang, T.; Wei, Y.; Koh, M. J. Photoinduced Nickel-Catalyzed Deaminative Cross-Electrophile Coupling for $C(sp^2)$–$C(sp^3)$ and $C(sp^3)$–$C(sp^3)$ Bond Formation. *ACS Catal.* **2021**, *11*, 6519–6525. (c) Kaur, J.; Shahin, A.; Barham, J. P. Photocatalyst-Free, Visible-Light-Mediated $C(sp^3)$–H Arylation of Amides via a Solvent-Caged EDA Complex. *Org. Lett.* **2021**, *23*, 2002–2006. (d) Polites, V. C.; Badir, S. O.; Keess, S.; Jolit, A.; Molander, G. A. Nickel-Catalyzed Decarboxylative Cross-Coupling of Bicyclo[1.1.1]pentyl Radicals Enabled by Electron Donor-Acceptor Complex Photoactivation. *Org. Lett.* **2021**, 23, 4828–4833. (e) Uchikura, T.; Fujii, T.; Moriyama, K.; Akiyama, T. Visible-Light Driven, Metal-Free Hydroalkylation of Alkenes Mediated by Electron Donor-Acceptor Complex Using Benzothiazolines. *Bull. Chem. Soc. Jpn.* **2021**, *94*, 2962–2966. (f) Kammer, L. M.; Badir, S. O.; Hu, R.-M.; Molander, G. A. Photoactive Electron Donor-Acceptor Comolex Platform for Ni-Mediated $C(sp^3)$–$C(sp^2)$ Bond Formation. *Chem. Sci.* **2021**, *12*, 5450–5457. (g) Badir, S. O.; Lipp, A.; Krumb, M.; Cabrera-Afonso, M. J.; Kammer, L. M.; Wu, V. E.; Huang, M.; Csakai, A.; Marcaurelle, L. A.; Molander, G. A. *Chem. Sci.* **2021**, *12*, 12306–12045. (h) Saux, E. L.; Zanini, M.; Melchiorre, P. Photochemical Organocatalytic Benzylation of Allylic C–H Bonds. *J. Am. Chem. Soc.* **2022**, *144*, 1113–1118. (i) Cabrera-Afonso, M. J.; Granados, A.; Molander, G. A. Sustainable Thioesterification via Electron Donor-Acceptor Photoactivation Using Thianthrenium Salts. *Angew. Chem. Int. Ed.* **2022**, *61*, e202202706. (j) Sharique, M.; Majhi, J.; Dhungana, R. K.; Kammer, L. M.; Krumb, M.; Lipp, A.; Romero, E.; Molander, G. A. A Practical and Sustainable Two-Component Minisci Alkylation via Photo-Induced EDA-Comolex Activation. *Chem. Sci.* **2022**, *13*, 5701–5706. (k) Zhou, W.; Wu, S.; Melchiorre, P. Tetrachlorophthalimides as Organocatalytic Acceptors for Electron Donor-Acceptor Complex Photoactivation. *J. Am. Chem. Soc.* **2022**, *144*, 8914–8919.

[7] For a review on photocatalyzed hydrogen atom transfer, see: (a) Capaldo, L.; Ravelli, D.; Fagnoni, M. Direct Photocatalyzed Hydrogen Atom Transfer (HAT) for Aliphatic C–H Bonds Elaboration. *Chem. Rev.* **2022**, *122*, 1875–1924. For selected examples of hydrogen atom abstraction from $C(sp^3)$–H by light driven generated aryl radical, see: (b) Jing, L.; Nash, J. J.; Kenttämaa, H. I. Correlation of Hydrogen-Atom Abstraction Reaction Efficiencies for Aryl Radicals with their Vertical Electron Affinities and the Vertical Ionization Energies of the Hydrogen-Atom Donors. *J. Am. Chem. Soc.* **2008**, *130*, 17697–17709. (c) Parasram, M.; Chuentragool, P.; Sarkar, D.; Gevorgyan, V. Photoinduced Formation of Hybrid Aryl Pd-Radical Species Capable of 1,5-HAT: Selective Catalytic Oxidation of Silyl Ethers into Silyl Enol Ethers. *J. Am. Chem. Soc.* **2016**, *138*, 6340–6343. (d) Chen, J.-Q.; Wei, Y.-L.; Xu, G.-Q.; Liang, Y.-M.; Xu, P.-F. Intramolecular 1,5-H Transfer Reaction of Aryl Iodides through Visible-Light Photoredox Catalysis: A Concise Method for the Synthesis of Natural Product Scaffolds. *Chem. Commun.* **2016**, *52*, 6455–6458. (e) Hokamp, T.; Dewanji, A.; Lübbesmeyer, M.; Mück-Lichtenfeld, C.; Würthwein, E.-U.; Studer, A. Radical Hydrodehalogenation of Aryl Bromides and Chlorides with Sodium Hydride and 1,4-Dioxane. *Angew. Chem. Int. Ed.* **2017**, *56*, 13275–13278. (f) Si, X.; Zhang, L.; Rudolph, M.; Asiri, A. M.; Hashmi, A. S. K. *Org. Lett.* **2020**, *22*, 5844–5849. (g) Kang, J.; Hwang, H. S.; Soni, V. K.; Cho, E. J. Direct $C(sp^3)$–N Radical Coupling: Photocatalytic C–H Functionalization by Unconventional Intermolecular Hydrogen Atom Transfer to Aryl Radical. *Org. Lett.* **2020**, *22*, 6112–6116.

[8] For examples of the phenoxide-driven photoreactions, see: (a) Liu, B.; Lim, C.-H.; Miyake, G. M. Light-Driven Intermolecular Charge Transfer Induced Reactivity of Ethynylbenziodoxol(on)e and Phenols. *J. Am. Chem. Soc.* **2018**, *140*, 12829–12835. (b) Guo, Q.; Wang, M.; Liu, H.; Wang, R.; Xu, Z. Visible-Light-Promoted Dearomative Fluoroalkylation of β-Naphthols through Intermolecular Charge Transfer. *Angew. Chem. Int. Ed.* **2018**, *57*, 4747–4751. (c) Liang, K.; Li, N.; Zhang, Y.; Li, T.; Xia, C. Transition-Metal-Free α-Arylation of Oxindoles via Visible-Light-Promoted Electron Transfer. *Chem. Sci.* **2019**, *10*, 3049–3053. (d) Liang, K.; Liu, Q.; Shen, L.; Li, X.; Wei, D.; Zheng, L.; Xia, C. Intermolecular Oxyarylation of Olefins with Aryl Halides and TEMPOH Catalyzed by the Phenolate Anion under Visible Light. *Chem. Sci.* **2020**, *11*, 6996–7002. (e) Wei, D.; Li, X.; Shen, L.; Ding, Y.; Liang, K.; Xia, C. Phenolate Anion-Catalyzed Direct Activation of Inert Alkyl Chlorides Driven by Visible Light. *Org. Chem. Front.* **2021**, *8*, 6364–6370. (f) Matsuo, K.; Yamaguchi, E.; Itoh, A. Halogen-Bonding-Promoted Photo-Induced C–X Borylation of Aryl Halide using Phenol Derivatives. *Chem. Rxiv*. DOI: 10.26434/chemrxiv-2022-glvkg.

[9] Yang, Q.-Q.; Liu, N.; Yan, J.-Y.; Ren, Z.-L.; Wang, L. Visible Light- and Heat-Promoted C–O Coupling Reaction of Phenols and Aryl Halides. *Asian J. Org. Chem.* **2020**, *9*, 116–120.

[10] (a) Filippini, G.; Nappi, M.; Melchiorre, P. Photochemical Direct Perfluoroalkylation of Phenols. *Tetrahedron* **2015**, *71*, 4535–4542. (b) Zhu, D.-L.; Jiang, S.; Young, D. J.; Wu, Q.; Li, H.-Y.; Li, H.-X. Visible-Light-Driven $C(sp^2)$–H Arylation of Phenols with Arylbromides Enabled by Electron Donor-Acceptor Excitation. *Chem. Commun.* **2022**, *58*, 3637–3640. (c) Li, H.-H.; Li, S.; Cheng, J. K.; Xiang, S.-H.; Tan, B. Direct Arylation of N-Heterocycles Enabled by Photoredox Catalysis. *Chem. Commun.* **2022**, *58*, 4392–4395. (d) Cuadros, S.; Rosso, C.; Barison, G.; Costa, P.; Kurbasic, M.; Bonchio, M.; Prato, M.; Filippini, G.; Dell'Amico, L. The Photochemical Activity of a Halogen-Bonded Complex Enables the Microfluidic light-Driven Alkylation of Phenols. *Org. Lett.* **2022**, *24*, 2961–2966.

[11] (a) Uchikura, T.; Hara, Y.; Tsubono, K.; Akiyama, T. Visible-Light-Driven C–S Bond Formation Based on Electron Donor–Acceptor Excitation and Hydrogen Atom Transfer Combined System. *ACS Org. Inorg. Au* **2021**, *1*, 23–28. (b) Li, T.; Liang, K.; Tang, J.; Ding, Y.; Tong, X.; Xia, C. A Photoexcited Halogen-Bonded EDA Complex of the Thiophenolate Anion with Iodobenzene for $C(sp^3)$–H Activation and Thiolation. *Chem. Sci.* **2021**, *12*, 15655–15661.

[12] For examples of Minisci-type alkyl radical addition to arenes, see: (a) Ueno, R.; Shirakawa, E. Base-Promoted Dehydrogenative Coupling of Benzene Derivatives with Amides or Ethers. *Org. Biomol. Chem.* **2014**, *12*, 7469–7473. (b) Rammal, F.; Gao, D.; Boujnah, S.; Gaumont, A.-C.; Hussein, A.-A.; Lakhdar, S. Visible-Light-Mediated C–H Alkylation of Pyridine Derivatives. *Org. Lett.* **2020**, *22*, 7671–7675. (c) Tian, H.; Yang, H.; An, G.; Li, G. Cross-Dehydrogenative Coupling of Strong $C(sp^3)$–H with *N*-Heteroarenes through Visible-Light-Induced Energy Transfer. *Org. Lett.* **2020**, *22*, 7709–7715.

[13] Screening of phenol catalysts is shown in Table S1, see Supporting Information.

[14] Screening of aryl halides is shown in Table S2, see Supporting Information.

[15] Hydrolysis of **6l** failed probably due to high electrophilicity of the aldehyde.

[16] Exact yield of **8** could not be estimated due to its volatility. The ^{2}H NMR spectra was shown in Figure S1 (See Supporting Information).

[17] The photon flux of the 450 nm blue LED was previously determined by standard ferrioxalate actinometry, see Ref 4. The detail of the method was shown in Supporting Information. Representative example of reference, see: Cismesia, M. A.; Yoon, T. P. Characterizing Chain Processes in Visible Light Photoredox Catalysis. *Chem. Sci.* **2015**, *6*, 5426–5434.

[18] Formation of EDA complex between **1a** and **3a-Na** was also observed by UV–Vis spectra (Figure S3, see Supproting Information). Although excitation corresponding this absorption was inhibition pathway, it was not decomposition pathway.

[19] Renny, J. S.; Tomasevich, L. L.; Tallmadge, E. H.; Collum, D. B. Method of Continuous Variations: Applications of Job Plots to the Study of Molecular Associations in Organometallic Chemistry. *Angew. Chem. Int. Ed.* **2013**, *52*, 11998–12013.

[20] The molecular orbitals of this halogen-bonding assisted EDA complex were also estimated by DFT calculation. Excitation from HOMO into LUMO+1 was supported in terms of overlapped orbitals and the energy values (Figure S6, see Supporting Information).